

**Phase separation of the electron-ion conducting layer on the surface of  $\text{TiP}_2\text{O}_7$  anode material for aqueous lithium rechargeable batteries**

Hanping Zhang,\* Yisen Zhou, Chenggang Li, Chao Yang and Tian Zhu

*Jiangsu Key Laboratory of Advanced Catalytic materials and technology, Changzhou University,*

*Changzhou, China.*

*\*Email - jinhongshi0001@163.com*

## Experimental

### 1. Synthesis of the electron-ion phase separation layer on the surface of the $\text{TiP}_2\text{O}_7$ matrix

The bulk of the  $\text{TiP}_2\text{O}_7$  sample was synthesized as follows:  $\text{TiO}_2$  and  $\text{NH}_4\text{H}_2\text{PO}_4$  were well mixed by ball milling in stoichiometric proportion and progressively heated to  $700\text{ }^\circ\text{C}$  at a heating rate of  $10\text{ }^\circ\text{C min}^{-1}$ . Then the mixture was calcined at this temperature for a further 6 h to yield the  $\text{TiP}_2\text{O}_7$  particles.

The synthesis of the phase separation samples is schematically shown in Fig. S1.



**Fig. S1 Schematic formation of the phase separation on the surface of the  $\text{TiP}_2\text{O}_7$  matrix.**

The as-prepared  $\text{TiP}_2\text{O}_7$  powder,  $\text{FeC}_2\text{O}_4$  and sucrose were dispersed in distilled water at series mass ratios to form emulsions, and then these emulsions were evaporated at  $80\text{ }^\circ\text{C}$  to form precursors. The precursors were thereafter progressively heated to  $700\text{ }^\circ\text{C}$  in nitrogen at a heating rate of  $10\text{ }^\circ\text{C min}^{-1}$  and calcined at this temperature for 6 h. During this progress, sucrose would be carbonized and  $\text{FeC}_2\text{O}_4$  would be decomposed to give rise of ferrous compounds. The ferrous compounds would afterwards react with the  $\text{TiP}_2\text{O}_7$  matrix to form a  $\text{Fe}_{0.5}\text{Ti}_2(\text{PO}_4)_3$  nano-layer. As a result, a phase separation occurred between the carbonized layer and the ferrous layer. Finally, an electron-ion phase-separated double conducting layer on the matrix of  $\text{TiP}_2\text{O}_7$  was created. The carbon-coated and  $\text{Fe}_{0.5}\text{Ti}_2(\text{PO}_4)_3$ -coated mono-layer samples were respectively prepared in the same way. All chemicals used were of analytical grade without any further treatment.

## 2.2. Structure Characterization and Electrochemical Measurements

Conventional powder XRD patterns were collected in the 10–80°  $2\theta$  range using a D/max 2500 PC with vertical goniometer and Cu K $\alpha$  radiation ( $\lambda=1.5406 \text{ \AA}$ ). Scanning electron microscope (SEM) images of the samples were collected on a JSM-6360LA at room temperature. Transmission electron microscopy (TEM) was performed on a JEM-2100 microscope at an operating voltage of 200 kV, equipped with a Gatan 832 CCD camera. Samples were prepared by dispersing a tiny amount of the sample in ethanol and sonicating it for 30 min. Then, a drop of the resulting suspension was deposited onto 300 mesh Formvar-coated copper grids (Ted Pella, Inc.). Thermo Gravimetric Analysis (TGA) measurement was carried out on a Thermogravimetric–differential thermal analyzer (TG 209 F3, Netzsch), recorded from 50 to 850 °C at a heating rate of 10 °C min<sup>-1</sup> in air atmosphere. The X-ray photoelectron spectroscopy (XPS) analysis was performed on a Perkin-Elmer PHI 550 spectrometer with Al K $\alpha$  X-radiation (1486.6 eV) as the X-ray source. The measurements were corrected by assigning a banding energy value of 285.0 eV to the C 1s as the reference line.

Cyclic voltammetric (CV) curves of the electrodes were recorded on an electrochemical workstation (CHI660D, Chenhua) at a scan rate of 0.5 mV s<sup>-1</sup>. A three-electrode cell was fabricated, in which a KCl-saturated calomel electrode and Pt sheet electrode were used as reference and counter electrode, respectively. 1 M Li<sub>2</sub>SO<sub>4</sub> aqueous solution was employed as the electrolyte. The work electrodes were made by the following steps: samples were mixed with acetylene black and poly(tetrafluoroethylene) (PTFE) in a weight ratio of 8:1:1 with the help of ethanol. The mixture was pressed into a film, and dried at 80 °C for 8 hours. Then the film was cut into a disk of about 5.0 mg and 0.33 cm<sup>2</sup> and pressed onto a piece of nickel grid.

A two-electrode cell was employed to characterize the impedance spectra. The cathode was composed of spinal  $\text{LiMn}_2\text{O}_4$  power, acetylene black, and PTFE, the composition and producing steps were in the same way with the  $\text{TiP}_2\text{O}_7$  anode. Both of the cathode and anode were cut into disks of about 5.0 mg and  $0.33 \text{ cm}^2$ . 1 M  $\text{Li}_2\text{SO}_4$  aqueous solution was employed as the electrolyte and the porous PP/PE membrane was used as separator. Impedance spectra were carried out on an EG&G M273 Potentiostat/galvanostat in conjunction with M5210 Lock-in amplifier electrochemical analysis system in the frequency range 0.01 Hz–100 kHz. The excitation voltage applied to the model cells was 10 mV.

The charge-discharge curves and cycle calendar life were traced on a cell tester (Neware) using a two-electrode cell with  $\text{LiMn}_2\text{O}_4$  as the cathode in 1 M  $\text{Li}_2\text{SO}_4$  aqueous solution. Rate performances were conducted at 0.8–1.7 V, the constant current rate shifted from 0.2 C to 50 C. 5 charge-discharge cycles were performed at each rate. All of the cyclic behaviors were collected at room temperature. The capacity is calculated based on the masses of all the contents of the active materials, including the masses of coaters.

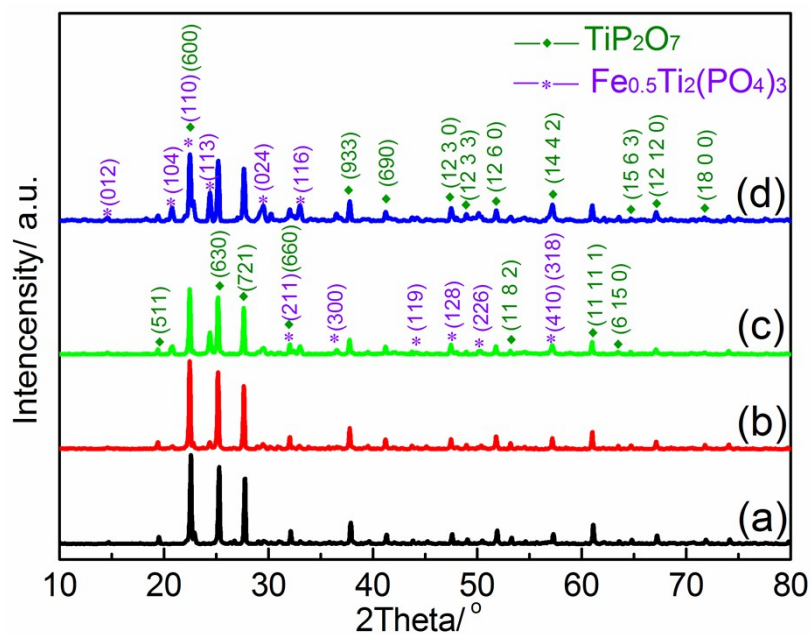


Fig. S2 XRD pattern of the  $\text{Fe}_{0.5}\text{Ti}_2(\text{PO}_4)_3$  covered  $\text{TiP}_2\text{O}_7$  with  $\text{FeC}_2\text{O}_4$  precursor to the  $\text{TiP}_2\text{O}_7$  mole ratio of (a) 0.01:9, (b) 0.1:9, (c) 0.2:9 and (d) 0.3:9, respectively.

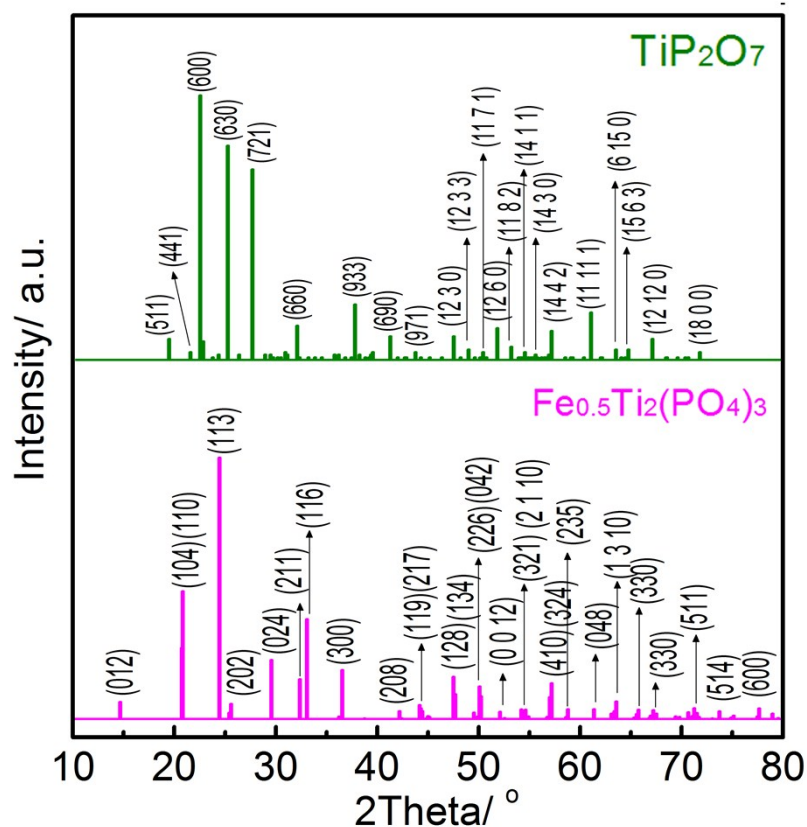
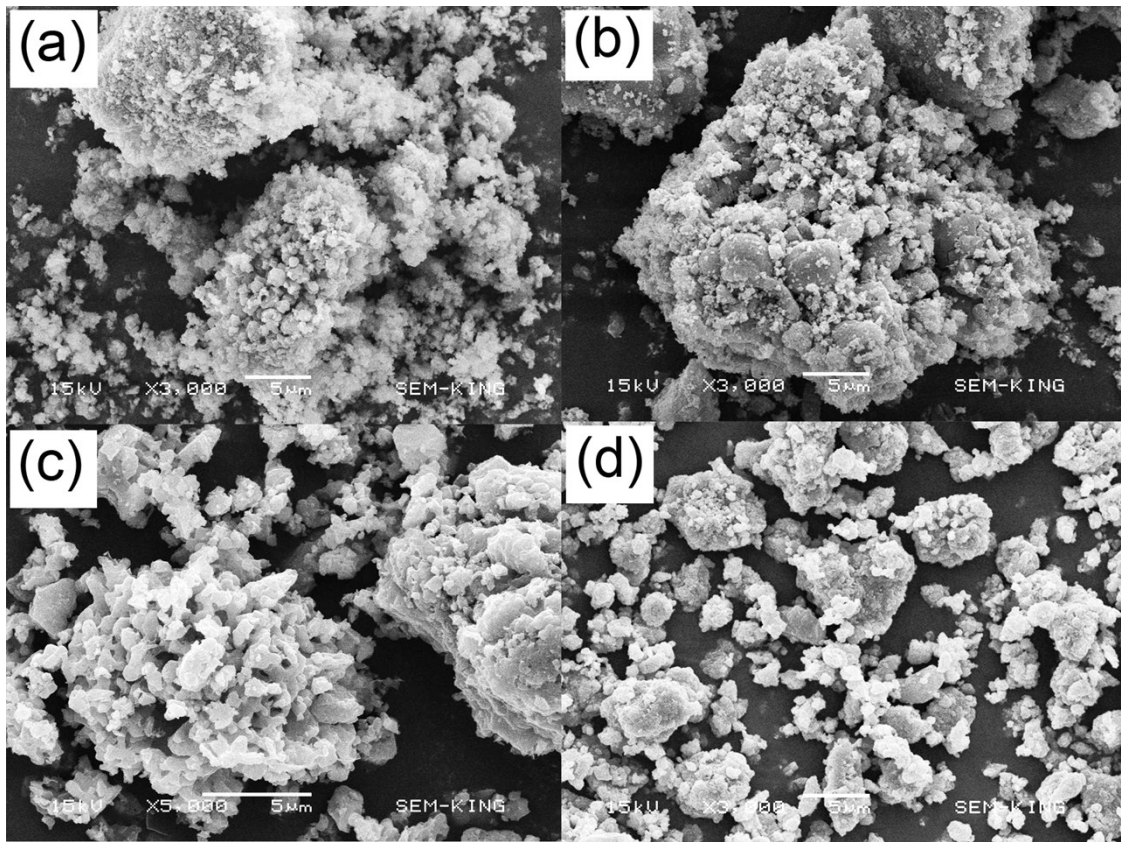
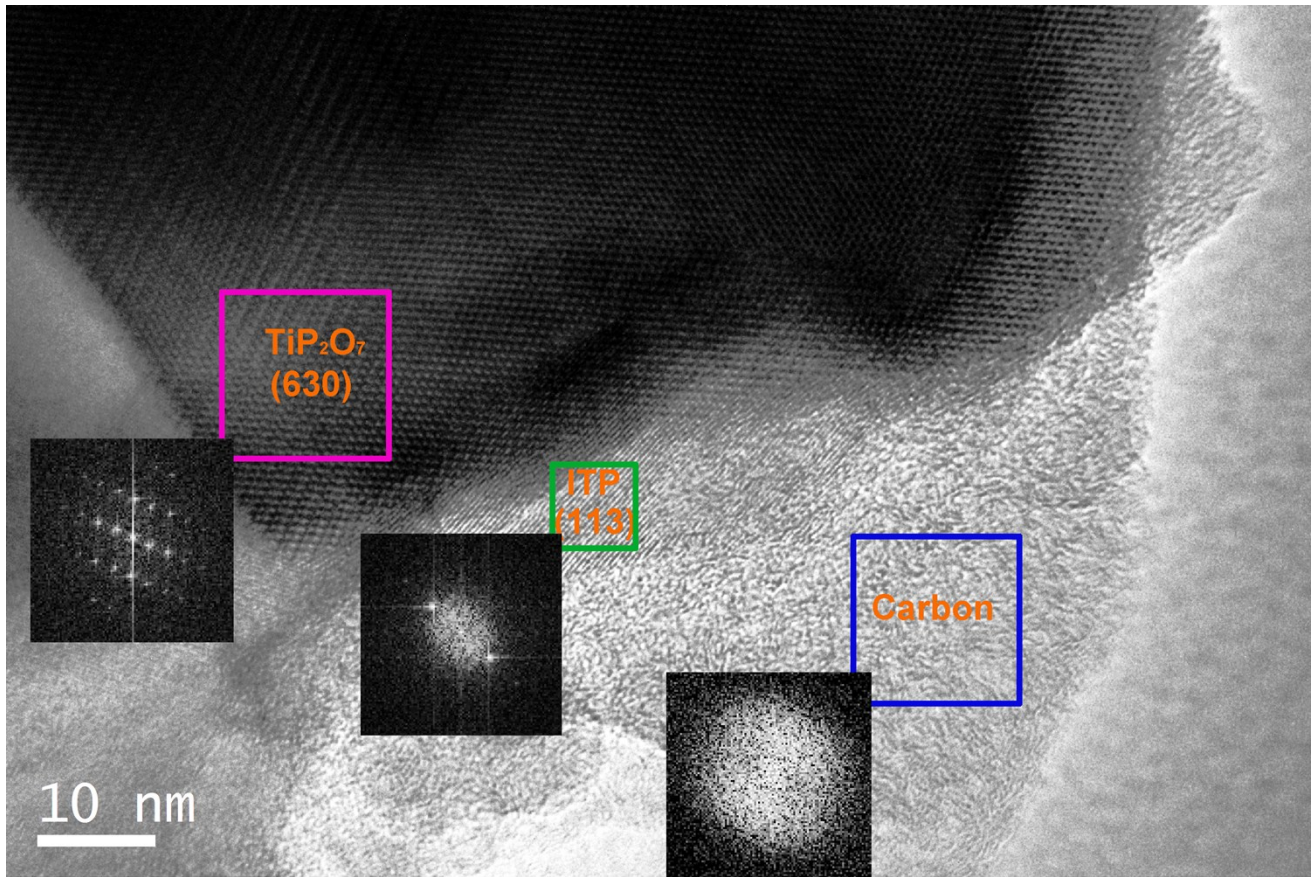


Fig. S3 XRD patterns of  $\text{Fe}_{0.5}\text{Ti}_2(\text{PO}_4)_3$  and  $\text{TiP}_2\text{O}_7$  delivered according to the PDF card.



**Fig. S4 SEM of (a) bared, (b) carbon coated, (c)  $\text{Fe}_{0.5}\text{Ti}_2(\text{PO}_4)_3$  coated and (d) carbon- $\text{Fe}_{0.5}\text{Ti}_2(\text{PO}_4)_3$  coated  $\text{TiP}_2\text{O}_7$ .**



**Fig. S5** The crystal lattice of the  $\text{Fe}_{0.5}\text{Ti}_2(\text{PO}_4)_3$  layer and the amorphous carbon covered on the matrix of  $\text{TiP}_2\text{O}_7$ .

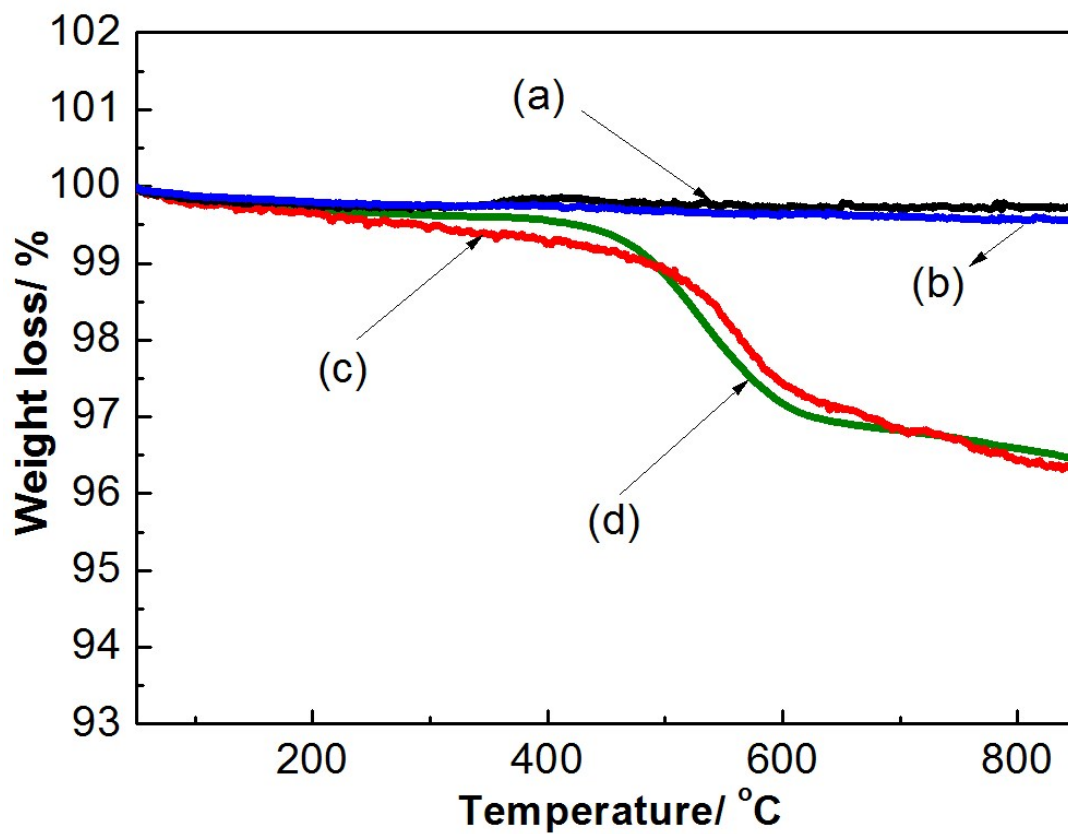
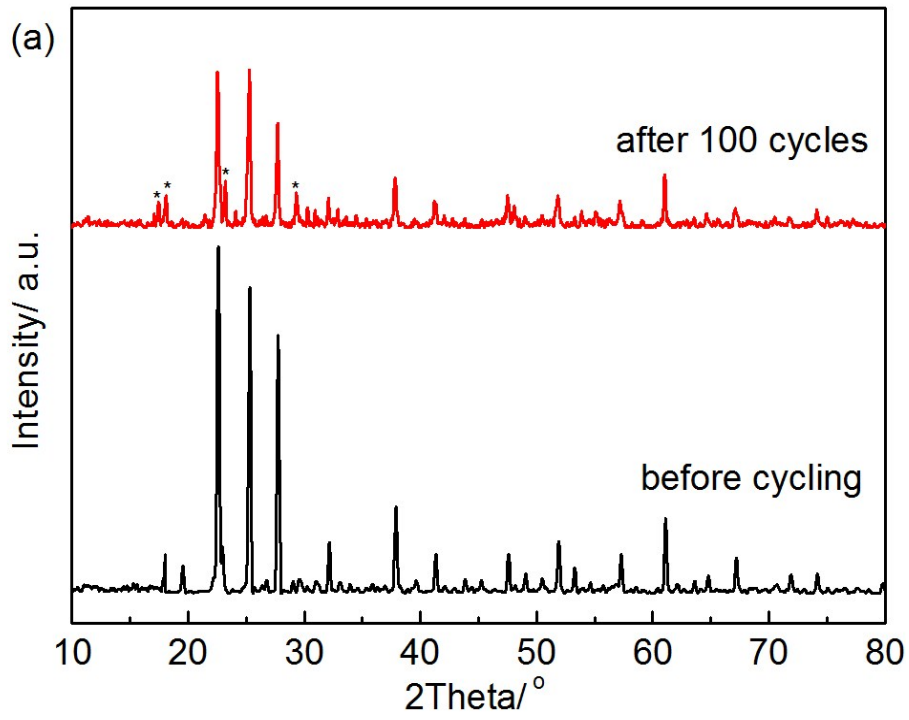
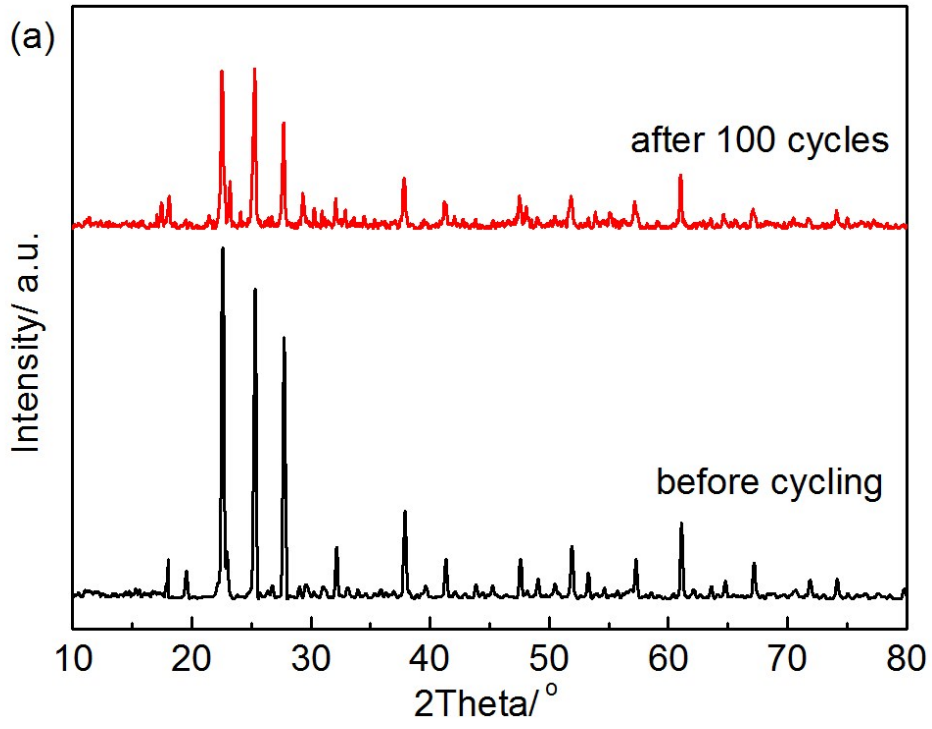
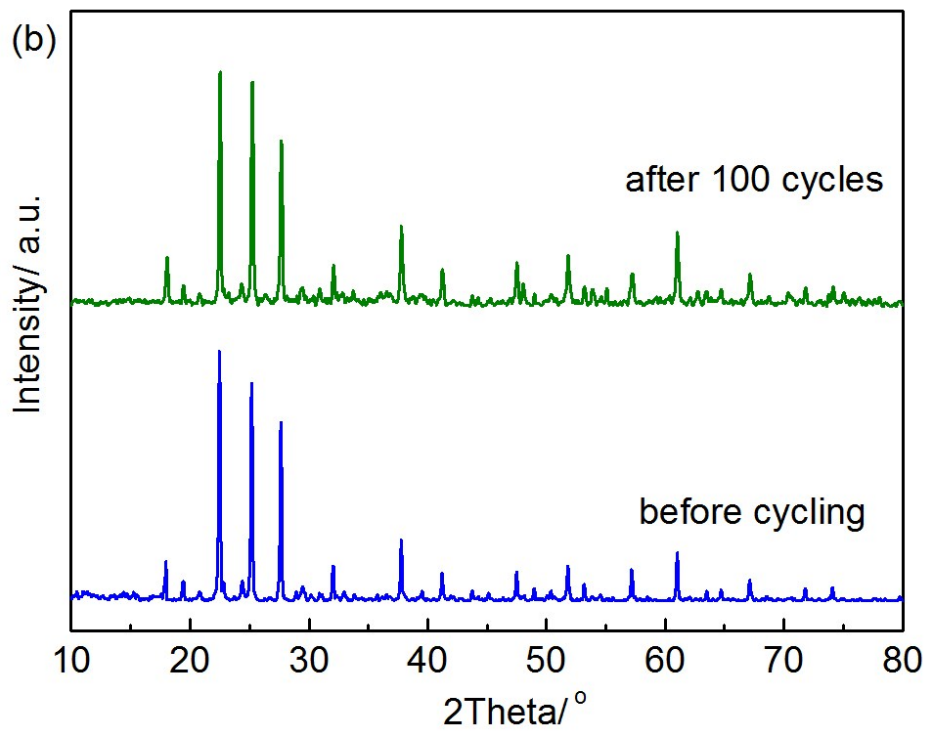


Fig. S6 TG of (a) bared, (b) Fe<sub>0.5</sub>Ti<sub>2</sub>(PO<sub>4</sub>)<sub>3</sub> coated, (c) carbon coated and (d) carbon-Fe<sub>0.5</sub>Ti<sub>2</sub>(PO<sub>4</sub>)<sub>3</sub> coated TiP<sub>2</sub>O<sub>7</sub>.







**Fig. S7 XRD patterns of (a) carbon coated and (b) carbon- $\text{Fe}_{0.5}\text{Ti}_2(\text{PO}_4)_3$  coated  $\text{TiP}_2\text{O}_7$  before and after 100 cycles.**

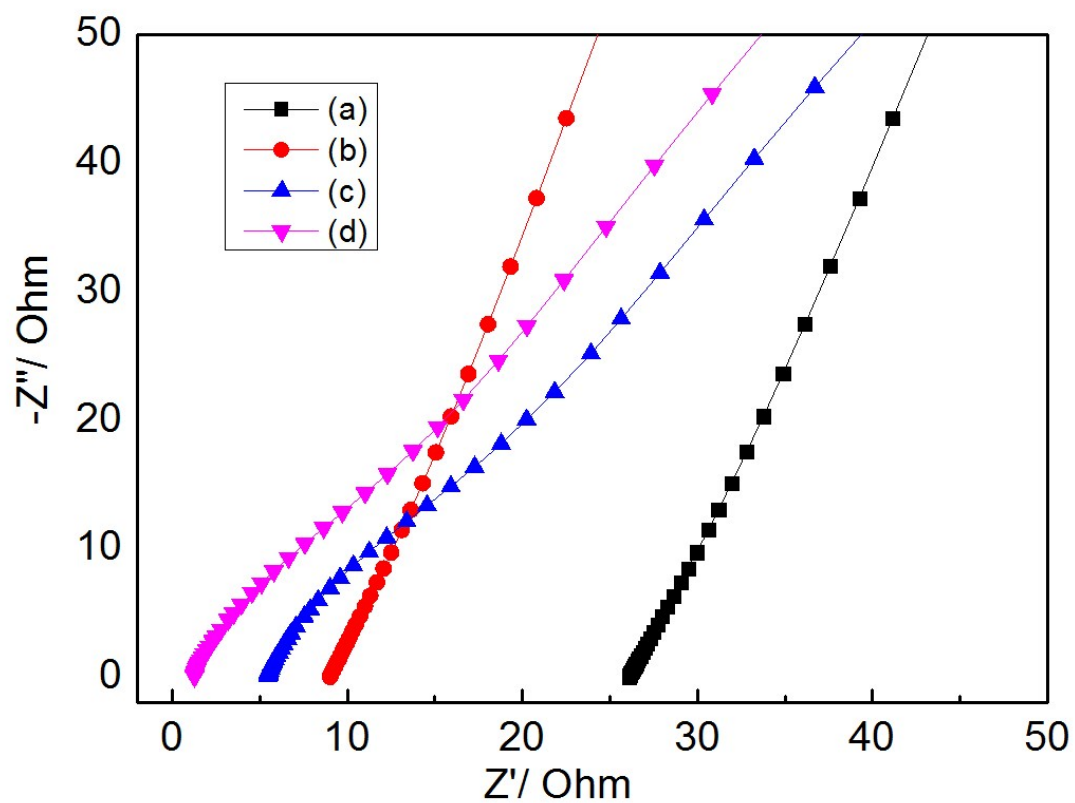
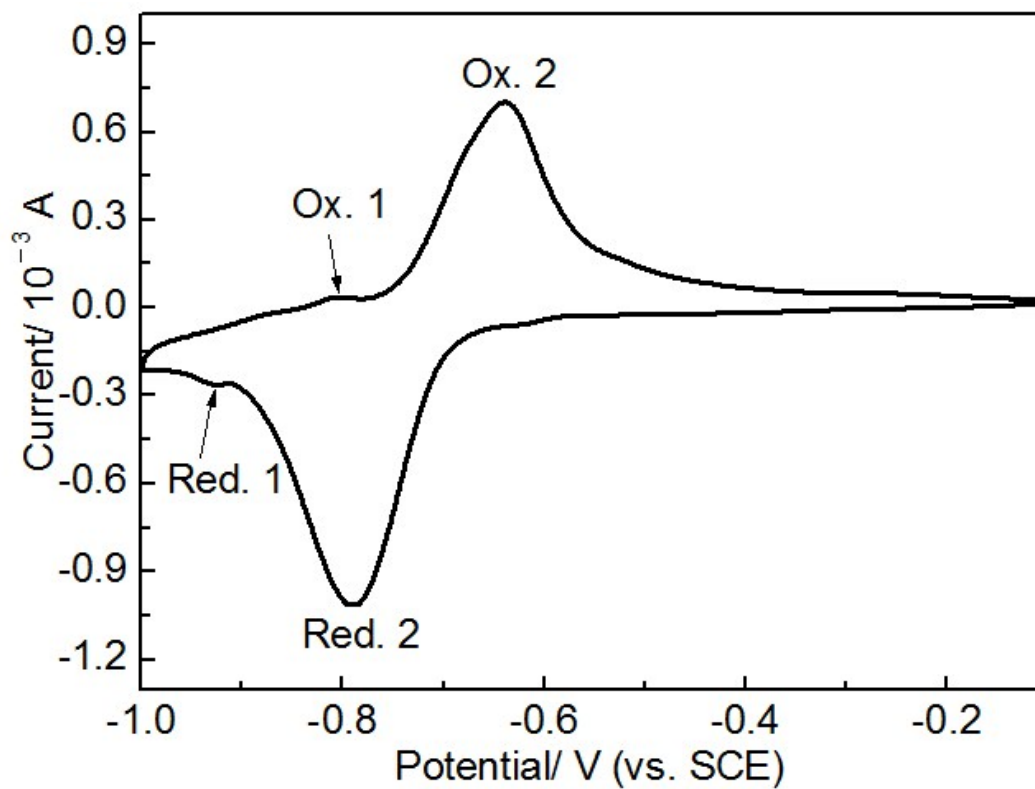


Fig. S8 Nyquist plots of the aqueous lithium batteries composed of  $\text{LiMn}_2\text{O}_4$  cathodes and (a) bared, (b) carbon coated, (c)  $\text{Fe}_{0.5}\text{Ti}_2(\text{PO}_4)_3$  coated and (d) carbon- $\text{Fe}_{0.5}\text{Ti}_2(\text{PO}_4)_3$  coated  $\text{TiP}_2\text{O}_7$  anodes.



**Fig. S9** CV curve of the carbon- $\text{Fe}_{0.5}\text{Ti}_2(\text{PO}_4)_3$  coated  $\text{TiP}_2\text{O}_7$  prepared at the  $\text{FeC}_2\text{O}_4$  precursor to the  $\text{TiP}_2\text{O}_7$  mole ratio of 0.3:9.

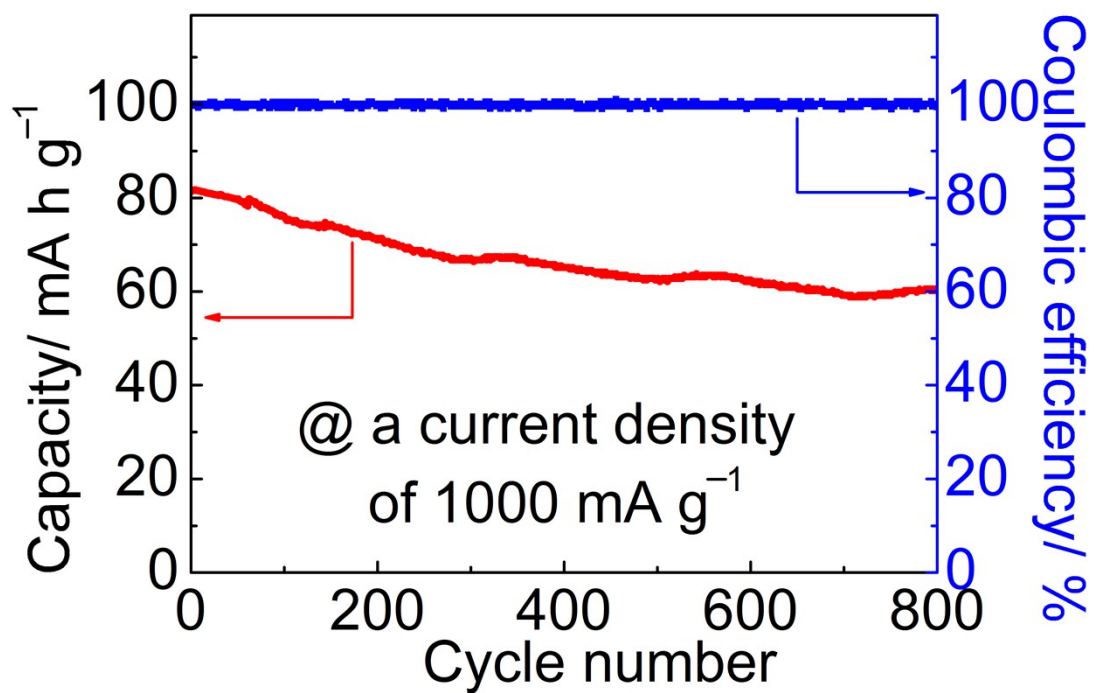


Fig. S10 Discharge capacity of the carbon-Fe<sub>0.5</sub>Ti<sub>2</sub>(PO<sub>4</sub>)<sub>3</sub> coated TiP<sub>2</sub>O<sub>7</sub> in the aqueous lithium battery with LiMn<sub>2</sub>O<sub>4</sub> as the cathode at 10 C rate.